Appl. Phys. B 66, 603–608 (1998)

Applied Physics B
Lasers
and Optics
© Springer-Verlag 1998

Ion strings for quantum gates

H.C. Nägerl, W. Bechter, J. Eschner, F. Schmidt-Kaler, R. Blatt

Institut für Experimentalphysik, Universität Innsbruck, Technikerstraße 25, A-6020 Innsbruck, Austria

Received: 6 August 1997/Revised version: 21 October 1997

Abstract. Crystal structures of calcium ions have been prepared in a linear Paul trap. The trapped ions are laser-cooled by simultaneous resonant excitation near 397 nm and 866 nm. Images of the fluorescing ions are obtained with a CCD camera and show the individual ions spatially resolved. Complex crystal structures of more than 60 ions have been observed whereas smaller crystals with up to 10 ions arrange in a linear string. Measured distances between the ions in strings of different lengths are in good agreement with expected values obtained from a harmonic trap potential. The application of a calcium ion string for quantum computation is discussed.

PACS: 32.80.Pj, 42.50.Vk

Ion traps have been shown to provide an ideal environment for isolated quantum systems such as a single, trapped and laser-cooled atoms. Ion storage has long been applied to ultra-high precision spectroscopy and the development of frequency standards [1]. More recently, single trapped ions have been used to demonstrate and test some of the intriguing features of quantum mechanics [2, 3]. In particular, both the internal electronic state and the motional state of a trapped ion can be modified using laser light. Decoherence of internal superposition states is nearly negligible even for very long interaction times. To explore these properties, several schemes have been proposed for the preparation of non-classical states of motion in a trap [4]. Their experimental realization [2] promises further improvement for the precision of spectroscopic measurements [5, 6]. With almost perfect control of the quantum state of a single ion, attention has turned to systems of few ions with well-controlled interactions between them. Manipulations of their overall quantum state include the preparation of entangled states that have no classical counterpart. The possibility of entangling massive particles opens up many prospects for new experiments including measurements with Bell states and GHZ states [7] which would allow for new tests of quantum mechanics. Moreover, entanglement of particles will allow one to study quantum measurements such as the investigation of decoherence processes [3, 8] in more detail.

A very exciting proposal is the application of linear ion traps and the collective quantum motion of a trapped string of ions for the realization of a quantum gate [9]. Quantum gates are the basic building blocks of a quantum computer and their operation relies fundamentally on the entanglement of internal degrees of freedom of the ions (electronic excitation) and their collective motion (vibrational excitation). A quantum computer works with quantum registers made up of quantum bits (qbits) which can be manipulated analogously to classical bits using gate operations. The quantum-mechanical analogue of a classical XOR gate, the so-called controlled-NOT gate operation, can be realized using a linear string of ions and a well-defined series of laser pulses to address different ions. It has been shown that a controlled-NOT gate operating on two ions is a realization of a universal quantum gate, so that in principle universal computations can be carried out using just the two-ion quantum gate and one-bit rotations [10]. The realization of these gate operations based on a string of ions would therefore be of fundamental interest and furthermore all basic algorithms could be tested using just a string of trapped ions.

Many species of ions have been used for ion trapping, and strings in linear traps have been experimentally demonstrated with Be^+ ions [11] and Mg^+ ions [12]. However, it was shown that $^{40}Ca^+$ is one of the most promising candidates for the realization of quantum gates, because of its mass, level structure, and transition frequencies and widths [13]. Furthermore, quantum gates require certain characteristics of the linear trap that have not been met in earlier experiments, in particular optical access from many directions.

In this paper, we report the first trapping of strings of $^{40}Ca^+$ ions in a linear trap, as a significant step towards the realization of a quantum gate. The novel trap that we use and describe in detail, has been designed especially for storing small numbers (up to a few tens) of $^{40}Ca^+$ ions with the aim of producing linear strings and using them as a quantum register. The paper is organized as follows. In Sect. 1 we present the requirements for an application of ion strings to quantum computation in the particular case of $^{40}Ca^+$. We also highlight the advantages of the specific choice of this ion. In Sect. 2 the experimental setup is described and in

Sect. 3 experimental results are presented and discussed. In the concluding section our next experimental steps towards the operation of a quantum gate are described.

1 $^{40}Ca^{+}$ for quantum computation

Quantum mechanical information is delicate and must be stored in systems which are essentially free of environmental perturbations. Any interactions with an environment, such as collisions with walls or surrounding atoms of background gas, have an effect similar to a measurement process in that they tend to alter or destroy the quantum-mechanical information by inducing decoherence. Furthermore, the necessity to manipulate quantum states in order to implement algorithms requires that the quantum information can be stored for times that are long enough to allow for coherent interaction of the ions with external fields. These requirements are all met by the ion storage technique and therefore that is why stored ions have been proposed for future use in quantum computation. In that spirit, a single laser-cooled Be^{+} ion has been used to demonstrate the manipulations necessary for the implementation of a controlled-NOT gate [14]. The single qbit quantum information (the so-called target bit) was stored in two hyperfine ground states of the Be^{+} while the other qbit (the so-called control bit) was encoded in the quantized vibration. The gate operations were realized with optical Raman transitions. Thus the potential of trapped ions for quantum bits has been clearly demonstrated. However, since in that experiment the control and target bit are internal and external states of the same single ion, it cannot be scaled up to realize a larger quantum register. Instead, several ions with controlled interaction between them are required. For that purpose, a promising choice would be to use a string of $^{40}Ca^{+}$ ions. Each ion in the linear string represents a qbit with the quantum information stored in a metastable optical transition. Gate operations involve one additional bit (the so-called bus bit) for which the common center-of-mass vibration of the ion string would be used.

The relevant energy levels of $^{40}Ca^{+}$ are shown in Fig. 1. All transitions can be driven by diode lasers, frequency-doubled diode lasers, or Ti:sapphire lasers. Optical cooling and detection of resonance fluorescence is achieved by simultaneous application of laser light at 397 nm and 866 nm. The $D_{3/2}$ and $D_{5/2}$ levels have lifetimes of about 1 s [15, 16] and together with the $S_{1/2}$ ground state they can be used to store quantum information. Performing a quantum computation with a string of trapped $^{40}Ca^{+}$ ions prepared in the vibrational ground state will require a number of laser pulses on the $S_{1/2}$ to $D_{5/2}$ transition to be applied coherently to individual ions in accord with the algorithm given by the computational problem. Determining which of the ions are left in the $S_{1/2}$ ground state will conclude the computational cycle and yield the output of the quantum computer. A necessary ingredient is therefore the ability to measure state populations with a 100% detection efficiency. This is routinely done with trapped ions using the electron shelving technique [17–19] and can be realized with $^{40}Ca^{+}$ by exciting the ion to the $D_{5/2}$ state. Subsequent probing on the $S_{1/2}$ to $P_{1/2}$ transition results in fluorescence being either generated or not, indicating with certainty whether the ground state is populated or not.

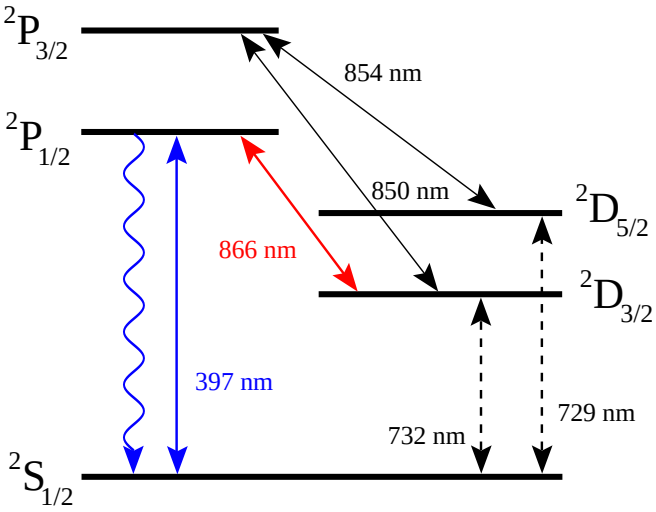

Fig. 1. Level scheme of $^{40}Ca^{+}$

This operation of quantum gates, as proposed by Cirac and Zoller [9], also requires the trapped string of ions to be cooled to the ground state of their collective vibrational motion. This cannot be achieved with cooling on the allowed transitions only but requires additional cooling techniques such as Raman cooling or sideband cooling with coupled transitions. A discussion of these and their experimental demonstration with *single* ions is given in [20–22]. With the transitions available in $^{40}Ca^{+}$, both advanced cooling techniques are possible. In particular, simultaneous excitation of the low-energy vibrational sideband of the $S_{1/2}$ to $D_{5/2}$ transition at 729 nm, and the $D_{5/2}$ to $P_{3/2}$ transition near 854 nm, would provide efficient sideband cooling to the motional ground state of the ion string.

It is clear that coherent manipulation of the $^{40}Ca^{+}$ ions requires a highly stabilized laser for the S–D transition near 729 nm. Decoherence will set in on a time scale proportional to the inverse laser bandwidth and limit the number of coherent manipulations that are possible. With the present laser system, already several gate operations could be performed. Decoherence of the qbits during their manipulation could be further suppressed by using ground state Zeeman coherences which would be controlled via radio-frequency techniques and Raman excitations [13, 14]. Another possibility is to store the quantum information in superpositions of the two metastable D states. At the expense of employing an additional laser source near 850 nm, phaselocked to the 854 nm laser with, for example, a comb generator [23], many coherent manipulations then become possible using optical transitions.

2 Trap design, laser sources, and fluorescence detection

Linear traps for ion clouds or for a few laser-cooled ions have been investigated by many groups [11, 12, 24–26]. For computational purposes the linear trap should be optimized to hold linear strings of ions and the motion should be as harmonic as possible to allow for optimal cooling. In addition, optical access to the trap should be very good to ensure optimal imaging and application of the manipulating beams

which address individual ions. This in turn requires that the mean spacing between the ions should be such that a laser beam near 729 nm can be easily focused on any chosen ion without exciting adjacent ones.

Figure 2 shows the realized trap, which is mounted inside the UHV system. It consists of 4 stainless steel rods with a diameter of 0.6 mm at a center distance of 2 mm, diagonally connected to generate the quadrupole rf field for dynamic confinement in the x–y plane perpendicular to the trap z axis. Two ring electrodes with dc potentials serve as the axial endcaps for longitudinal static confinement. The endcap rings have an inner diameter of about 4 mm and the spacing between them is 10 mm. The rf drive frequency ($\Omega/2\pi = 18$ MHz) is amplified, resonantly enhanced by a helical resonator (loaded $Q \approx 250$) and coupled to one pair of rod electrodes with the other pair grounded. The alternating rf potential yields a trap (quasi-)potential with secular frequencies of up to $\omega_r = \omega_{x,y} \approx 1.2$ MHz. For longitudinal confinement, dc voltages between 20 V and 400 V are applied to the rings resulting in an axial vibrational frequency ω_z of between 20 kHz and 400 kHz. At standard operating conditions, ω_z is about 180 kHz. Numerical calculations reveal that the axial static trap potential is a very good approximation to a harmonic potential. According to these calculations, within a distance in the z direction of about 50 μm from the trap centre, contributions of higher-order potentials are as small as 2×10^{-6}. For the frequencies $(\omega_r, \omega_z) = (1.2, 0.2)$MHz we obtain the Lamb–Dicke parameters $\eta_{r,z} = \sqrt{\hbar k^2/2m\omega_{r,z}} = (0.09, 0.22)$ for the transition near $\lambda = 729$ nm and $(\eta_r, \eta_z) = (0.16, 0.4)$ for the λ = 397 nm cooling transition. Here, $k = \sin\alpha 2\pi/\lambda$ is the effective wavevector of the light beam (applied at an angle $\alpha = 45°$ with respect to the r and z axes) and $m = 40$ amu denotes the mass of the Ca^+ ion. The rms size $\langle q\rangle = \sqrt{\hbar/2m\omega_q}$ of the ground state wavepacket corresponds to $(\langle r\rangle, \langle z\rangle) = (10, 25)$ nm. Within the Doppler cooling limit $E_D = \hbar\Gamma/2$, the mean vibrational quantum numbers of $(\langle n_r\rangle, \langle n_z\rangle) \approx (8, 50)$ are reached.

In order to achieve optical cooling in all dimensions, the ions are illuminated by laser light from the $(x, y, z) = (0, 1, -1)$ and the $(x, y, z) = (-1, 0, -1)$ direction. The emitted fluorescence light at 397 nm is collected simultaneously in opposite directions (along x) and recorded with a photomultiplier and a CCD camera, respectively. For the CCD camera, we use an $f/1$ optics with 40-fold magnification and an overall photon detection efficiency of 10^{-3}. Ca^+ ions are produced from a weak atomic beam by impact ionization from an electron beam focused to the trap centre. The magnetic field is controlled by Helmholtz coils in all dimensions.

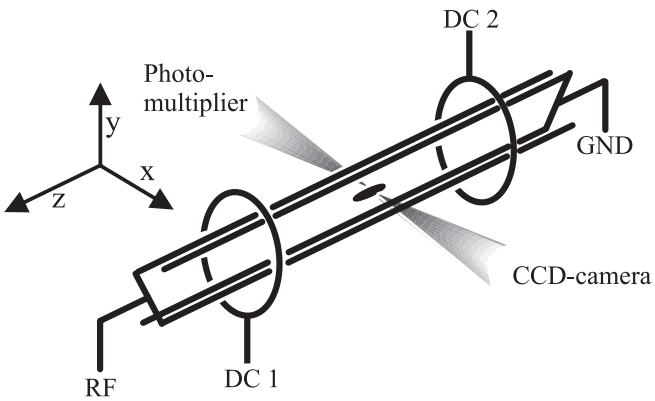

Fig. 2. Setup of linear ion trap

For excitation and manipulation of the trapped ions, solid-state and diode laser sources near 397 nm, 866 nm, 729 nm, and 854 nm are used. In order to generate the light at 397 nm, a Ti:sapphire ring laser is radio-frequency stabilized to an external cavity resulting in an rms linewidth of 250 kHz and a long-term drift stability of a few MHz/h. The output of up to 1.5 W at 793 nm is frequency doubled using an LBO crystal inside an external enhancement resonator. Typically, 25–30 mW of light near 397 nm is coupled with a fiber to the ion trap located on a different optical table. The fiber output of 5 mW is spatially filtered and allows for stable optical adjustment. About 15 mW of light at 866 nm is generated with an external-grating cavity diode laser in a Littrow arrangement. This laser is locked to a temperature-stabilized cavity yielding an rms linewidth of about 30 kHz. Thus, a low drift rate (few MHz/h) and a sufficient short-term stability of the diode laser is achieved. About 50 mW of light near 729 nm is generated with a second Ti:sapphire laser and is also fiber-coupled to the ion trap. This laser has been radio-frequency stabilized to an external cavity and provides a bandwidth near 10 kHz. Another diode laser with an external grating cavity produces 15 mW of light at 854 nm with a free-running bandwidth of 1 MHz. Stable and uninterrupted locking of all lasers has been accomplished for more than 5 h. The wavelengths of the lasers can be monitored with wavemeters, and for the laser sources at 397 nm, 866 nm, and 854 nm we obtain optogalvanic signals from a hollow cathode lamp. Laser frequencies and intensities are computer-controlled by acousto-optical modulators.

3 Experimental results

A typical experimental run starts with the preparation of a large cloud of ions. Ions are generated with the oven and electron gun operating, and the alignment of the laser beams with respect to the cloud is optimized. The laser frequencies are set to optimal cooling. Optionally, background gas cooling can be used by simply switching off the ion getter pump. The oven and electron gun are then switched off, and the getter pump is switched on again. The following procedure depends on the ordered structures to be produced. For large crystal structures, it is preferable to block the laser at 397 nm for several minutes. Radio-frequency heating of the extended cloud [27, 28] then results in a reduction in the cloud size, and when the laser is switched on again with the detuning chosen correctly, a large crystal ionic structure is usually obtained. We observed structures with more than 60 ions. An example is shown in Fig. 3 where the ions order themselves in opposing pairs of perpendicular orientation. Note the bright central spots in Fig. 3, which are due to two ions contributing to the fluorescence light in this particular line of sight.

Crystallization of the cloud can also be observed in a spectroscopic measurement [12]. This is shown in Fig. 4 where the fluorescent light, detected with the photomultiplier tube, is recorded as a function of the detuning near 397 nm. The detuning is scanned into resonance from the

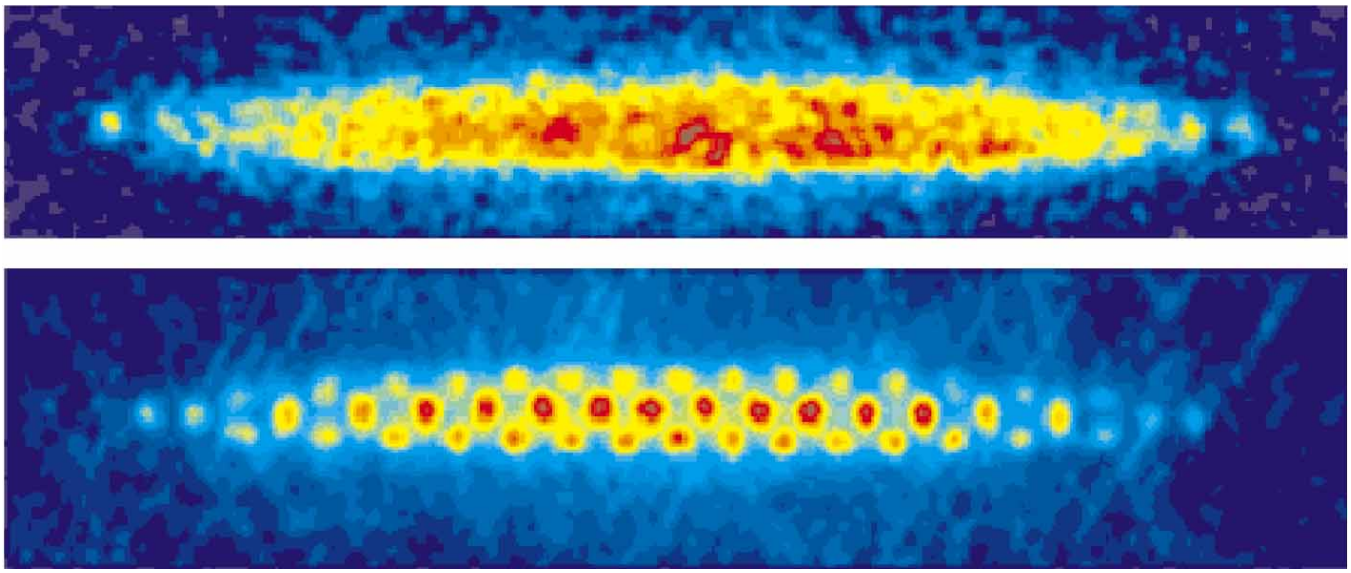

Fig. 3. *Upper part*: large hot ion cloud consisting of 62 ions, laser detuning not optimized for cooling (cf. Fig. 4a). *Lower part*: same sample for optimized optical cooling (cf. Fig. 4b), ion crystal consists of 62 ions. Note that the bright central spots represent the overlapping light of two ions. The total length of this ion crystal is 180 μm at $\omega_z = 195 \pm 5$ kHz

low-frequency side (from left to right in Fig. 4). Far below resonance (see (a) in Fig. 4) the fluorescence intensity increases as observed for a hot ion cloud (see upper part of Fig. 3). Laser cooling is not efficient because of the large detuning. At a certain detuning closer to resonance, crystallization shows up as a sharp feature in the spectrum which is the result of the sudden change from the Doppler-broadened cloud to a crystal. The fluorescence response of the crystal is similar to the excitation spectrum of a single laser-cooled ion. The sharp feature at the right of Fig. 4 indicates again the change to a cloud-like behavior, i.e. the melting of the ion crystal. The decrease of fluorescence

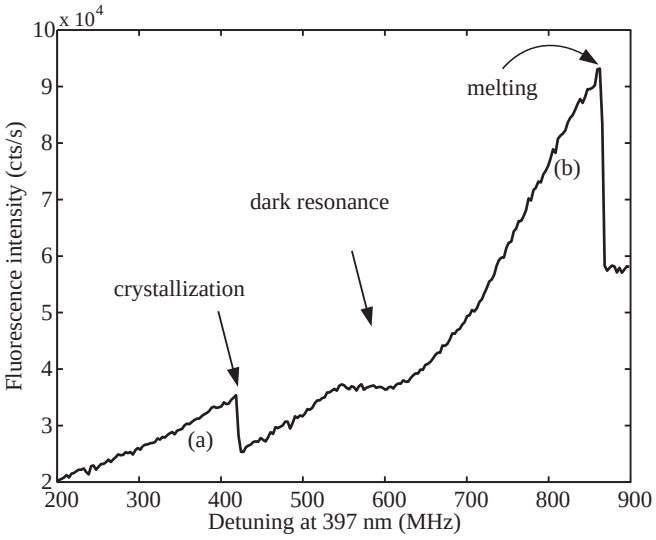

Fig. 4. Crystallization and melting of an ion cloud is observed when the cooling laser is tuned across the atomic resonance. The line shape to the left and to the right of the sharp features corresponds to a Doppler-broadened (cloud-like) spectrum, whereas the central part corresponds to a crystalline state. The upper part of Fig. 3 was taken at a detuning marked with (a), the lower part of Fig. 3 was taken at the detuning marked with (b)

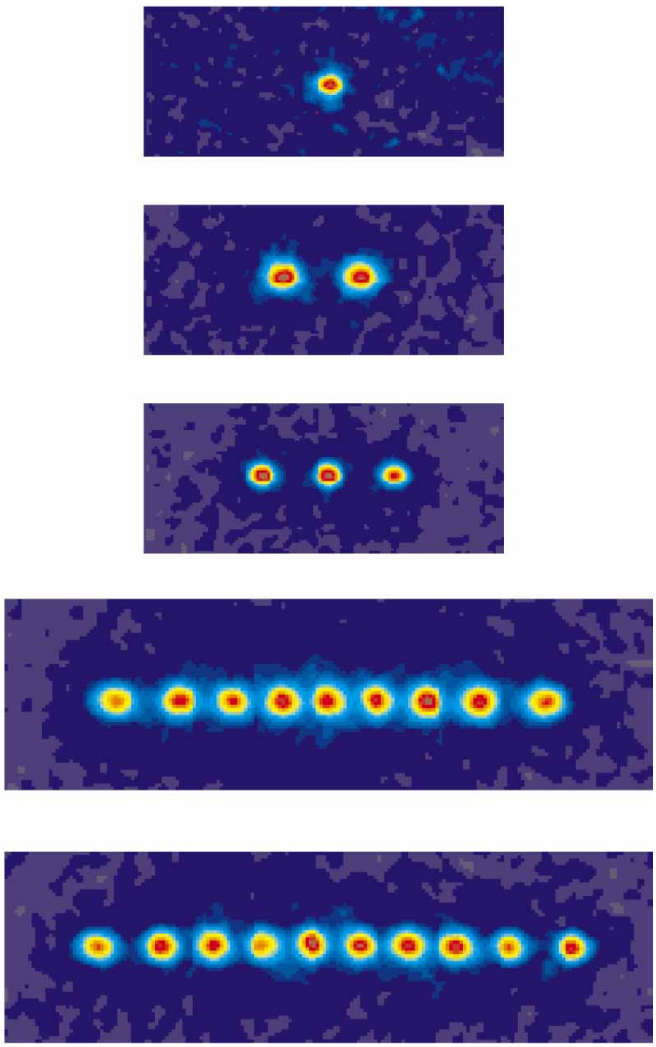

Fig. 5. Examples of some small linear strings of ions. The average distance between two ions is about 10 μm. The exposure time for the CCD camera was 1 s. The measured resolution of the imaging system consisting of the lens and CCD camera is better than 4 μm

light in the central part of the spectrum indicates a dark resonance in Ca^+ [29] which is broadened by the cooling laser.

For the trap parameters indicated above and the current trap design, ion numbers larger than 10 result in three-dimensional ordered structures. Smaller ion numbers and subsequently linear strings can be prepared by using heating procedures to reduce the ion number further. This is achieved either by applying blue detuned laser radiation on the 397 nm transition (laser heating) or by application of a radio frequency tuned to the secular vibration frequency of the ions. Since laser heating acts only on the ^{40}Ca isotope, the probability of other Ca^+ isotopes staying trapped is increased. These ions do not interact with the laser light and show up as non-fluorescing lattice sites in the crystal.

For single ions or for small strings of up to 5 ions it is easier experimentally to load them directly. This is achieved with the lasers set to optimal cooling, the oven operating continuously and the electron gun being pulsed for a few seconds. Images of the fluorescing ions are then readily obtained with the CCD camera with a spatial resolution of 4 μm. Several examples are shown in Fig. 5. The images were taken with an exposure time of 1 s and a spatial average is taken over 5 pixels which corresponds to about 2.5 μm. Note that the background light is subtracted to obtain the images.

For the realization of a two-bit quantum gate, individual ions have to be addressed by a laser beam. In a harmonic linear trap a single parameter, the trap frequency ω_z, suffices to describe the distances between the ions of a string, which allows one to calculate the expected positions of the ions. For up to 4 ions analytical results can be given, and for larger strings numerical results are readily derived [13]. Figure 6 shows a comparison of the experimental results with numerical calculations based on a value of ω_z = 181 kHz. Note that the deviations of the experimental values from the calculated positions are smaller than the optical resolution of the imaging system. These systematic deviations arise since most of the data were obtained during different experimental runs which required renewed loading of the trap. This procedure (calcium atomic beam and electron impact ionization) causes stray surface potentials on the electrodes owing to patch effects, which in turn modify the trap frequency ω_z slightly. In fact, each measurement in Fig. 6 (i.e. each string) could be individually fitted and an individual trap frequency could be assigned resulting in even better agreement with theory. However, the data presented in Fig. 6 prove that even a single value of the longitudinal trap frequency suffices to describe the ion positions well within the resolution of our optical system and, in particular, accurately enough to allow the steering of the addressing laser. Furthermore, the average distances in the order of 10–20 μm should be sufficient to focus radiation near 729 nm onto the individual ions.

The trap frequency ω_z was also measured directly. For this, a frequency signal was applied to the axially confining rings and tuned across the frequency range around ω_z. On resonance, the collective axial motion is excited and the ions heat up, which results in blurred pictures on the CCD camera. The observed values of ω_z are in good agreement with those calculated from the ion distances. Furthermore, from the well-resolved resonances we expect to be able to selectively excite the center-of-mass vibration in both sideband cooling and gate operation, without coupling into other modes of vibration.

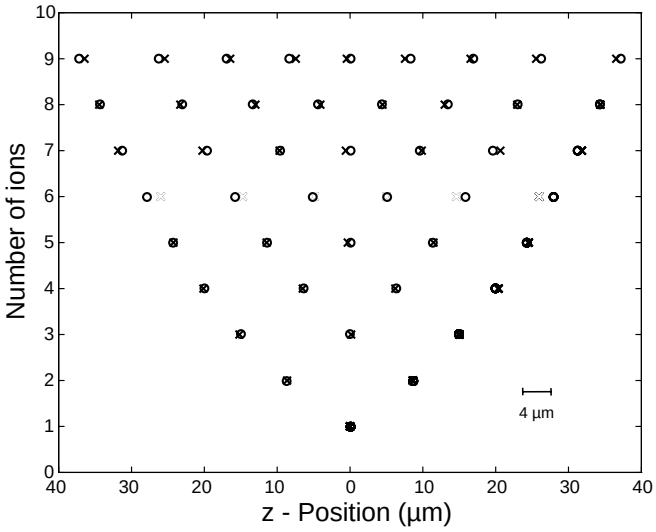

Fig. 6. Measured positions (x) of ions in strings of indicated number (1–9), compared with values (o) from analytic and numeric calculations using an axial frequency of $\omega_z = 181$ kHz. No experimental data were taken for 6 ions. The deviations are within the 4-μm resolution of the imaging system indicated by the horizontal bar

4 Conclusions and outlook

We have built a linear ion trap optimized for trapping a small number of $^{40}Ca^+$ ions and performing quantum gate operations between them. We have shown how strings of Ca^+ ions in this trap can be laser cooled and we observed them crystallize in a linear string. Using a CCD camera, we have been able to image the individual ions with high spatial resolution. The distances measured between the ions agree with analytically and numerically calculated values based on a harmonic trap potential. Also, the directly measured frequency of axial vibration is consistent with the value of ω_z obtained from the ion positions. Addressing individual ions will be achieved using an acousto-optic deflector driven by appropriate radio frequencies which can be derived from the distance measurements above.

The agreement between the expected and measured trap characteristics is encouraging for a future application of the $^{40}Ca^+$ strings as a quantum register. With additional cooling schemes it will be possible to reach the vibrational ground state [20–22] and then the ion strings can be applied to perform a quantum gate operation. Currently, the laser near 729 nm is being stabilized to an ultrahigh-finesse resonator to provide the frequency stability which is ultimately necessary for multiple gate operations.

Acknowledgements. This work is supported by the Fonds zur Förderung der wissenschaftlichen Forschung (FWF) under contract number P11467-PHY and in parts by the TMR networks “Quantum Information” (ERB-FMRX-CT96-0087), and “Quantum Structures” (ERB-FMRX-CT96-0077).

References

1. R. Blatt: In Atomic Physics **14**, ed. by D.J. Wineland, C.E. Wieman, S.J. Smith (AIP, New York 1995), pp. 219
2. D.M. Meekhof, C. Monroe, B.E. King, W.M. Itano, D.J. Wineland: Phys. Rev. Lett. **76** 1796 (1996)
3. C. Monroe, D.M. Meekhof, B.E. King, D.J. Wineland: Science **272**, 1131 (1996)
4. J.I. Cirac, A.S. Parkins, R. Blatt, P. Zoller: Adv. At. Molec. Opt. Phys. **37**, p. 238 (1996)
5. W.M. Itano, J.C. Bergquist, J.J. Bollinger, J.M. Gilligan, D.J. Heinzen, F.L. Moore, M.G. Raizen, D.J. Wineland: Phys. Rev. A **47**, 3554 (1993)
6. J.J. Bollinger, W.M. Itano, D.J. Wineland, D.J. Heinzen: Phys. Rev. A **54**, R4649 (1996)
7. D.M. Greenberger, M.A. Horne, A. Shimony, A. Zeilinger: Am. J. Phys. **58**, 1131 (1990); N.D. Mermin: Phys. Today (June, 9 1990)
8. W.H. Zurek: Phys. Today (October, 36 1991)
9. J.I. Cirac, P. Zoller: Phys. Rev. Lett. **74**, 4091 (1995)
10. D.P. DiVincenzo: Phys. Rev. A **51**, 1015 (1995)
11. M.G. Raizen, J.M. Gilligan, J.C. Bergquist, W.M. Itano, D.J. Wineland: Phys. Rev. A **45**, 6493 (1992)
12. I. Waki, S. Kassner, G. Birkl, H. Walther: Phys. Rev. Lett. **68**, 2007 (1992)
13. A. Steane: Appl. Phys. B **64**, 623 (1997)
14. C. Monroe, D.M. Meekhof, B.E. King, W.M. Itano, D.J. Wineland: Phys. Rev. Lett. **75**, 4714 (1995)
15. T. Gudjons, B. Hilbert, P. Seibert, G. Werth: Europhys. Lett. **33**, 595 (1996)
16. M. Knoop, M. Vedel, F. Vedel: Phys. Rev. A **52**, 3763 (1995)
17. W. Nagourney, J. Sandberg, H. Dehmelt: Phys. Rev. Lett. **56**, 2797 (1986)
18. Th. Sauter, W. Neuhauser, R. Blatt, P.E. Toschek: Phys. Rev. Lett. **57**, 1696 (1986)
19. J.C. Bergquist, R. Hulet, W.M. Itano, D.J. Wineland: Phys. Rev. Lett. **57**, 1699 (1986)
20. C. Monroe, D.M. Meekhof, B.E. King, S.R. Jeffers, W.M. Itano, D.J. Wineland, P. Gould: Phys. Rev. Lett. **74**, 4011 (1995)
21. F. Dietrich, J.C. Bergquist, W.M. Itano, D.J. Wineland: Phys. Rev. Lett. **62**, 403 (1989)
22. I. Marzoli, J.I. Cirac, R. Blatt, P. Zoller: Phys. Rev. A **49**, 2771 (1994)
23. M. Kourogi, B. Widiystomoko, Y. Takeuchi, M. Ohtsu: IEEE J. Quantum Electron. **31**, 2120 (1995)
24. M.E. Poitzsch, J.C. Bergquist, W.M. Itano, D.J. Wineland: Rev. Sci. Instrum. **67**, 129 (1996)
25. P.T.H. Fisk, M.J. Sellars, M.A. Lawn, C. Coles: Appl. Phys. B **60**, 519 (1995)
26. J.D. Prestage, G.J. Dick, L. Maleki: J. Appl. Phys. **66**, 1013 (1989)
27. H.G. Dehmelt: Adv. At. Mol. Opt. Phys. **3**, 53 (1967); *ibid.* **5**, 109 (1969)
28. R. Blümel, C. Kappler, W. Quint, H. Walther: Phys. Rev. A **40**, 808 (1989)
29. I. Siemers, M. Schubert, R. Blatt, W. Neuhauser, P.E. Toschek: Europhys. Lett. **18**, 139 (1992)